Letters

Spread-Spectrum Frequency Modulation With Adaptive Three-Level Current Scheme to Improve EMI and Efficiency of Three-Level Boost DCM PFC

Moonhyun Lee, *Student Member, IEEE*, and Jih-Sheng Lai, *Life Fellow, IEEE*

***Abstract*—Discontinuous conduction mode controlled boosting power-factor-correction (PFC) converters suffer from high differential-mode electromagnetic interference (EMI) and require a large input filter due to high inductor current ripples at a single switching frequency. To remedy the shortcomings, a downward spread-spectrum frequency modulation (SSFM) is proposed in this letter. The SSFM can be used by boosting PFC converters for reduced EMI and improved efficiency. On top of the frequency modulation, a novel adaptive three-level current (ATC) scheme is devised with three-level boost PFC using multilevel capability to obtain further reductions of peak current and EMI amplitude. Analyses and experiments validate that the proposed SSFM and ATC scheme can bring improvements of EMI and efficiency at the cost of increased output-voltage ripple.**

***Index Terms*—Discontinuous conduction mode (DCM), electromagnetic interference (EMI), power-factor correction (PFC), spread-spectrum frequency modulation (SSFM), three-level boost.**

I. Introduction

DEPENDING on inductor current waveforms of boosting power-factor-correction (PFC) circuit operations, PFC control methods can be categorized into three—continuous conduction mode (CCM), discontinuous conduction mode (DCM), and critical conduction mode (CRM) [1]. Among the methods, DCM- and CRM-based boosting PFC converters have been employed in universal-voltage low-to-mid power applications because of the absence of reverse recovery by zero-current turn-ON, low-cost diode implementation, and low converter cost [2].

Boosting PFCs with DCM operate based on fixed switching frequency, while CRM control brings inherently time-varying operation frequency [3]. Due to the difference, DCM control can exclude zero-current-detection circuitry and exquisite switching-cycle control, achieving a simpler control structure. However, higher current peak/ripple and device current stresses are relative drawbacks compared to CRM method. Furthermore, differential-mode (DM) electromagnetic interference (DM-EMI) amplitudes from DCM are much higher than CRM since all the EMI-related energies are concentrated on a single frequency, causing increased size and weight of the input filter [4].

Manuscript received June 24, 2020; revised July 27, 2020; accepted August 4, 2020. Date of publication August 12, 2020; date of current version October 30, 2020. *(Corresponding author: Moonhyun Lee.)*

The authors are with the Future Energy Electronics Center (FEEC), Department of Electrical and Computer Engineering, Virginia Polytechnic Institute and State University, Blacksburg, VA 24061 USA (e-mail: leemh@vt.edu; laijs@vt.edu).

Color versions of one or more of the figures in this article are available online at https://ieeexplore.ieee.org.

Digital Object Identifier 10.1109/TPEL.2020.3016238

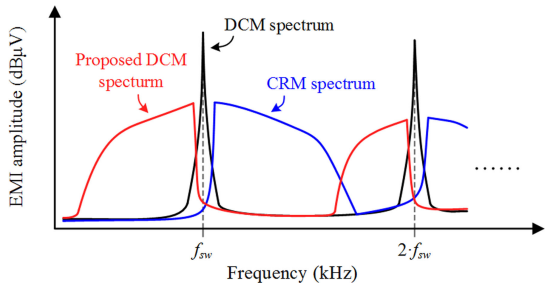

Fig. 1. Frequency spectrum by control method.

In recent years, an effective EMI reduction technique called spread-spectrum frequency modulation (SSFM) has been widely studied and adopted to power-electronic systems in various applications [5]–[7]. Major clients of SSFM method have been dc–dc converters, especially for resonant-type converters of which system characteristics are highly related to frequencies [5], [6]. With SSFM, the switching frequency can be distributed to the intended range so that critical EMI amplitudes can be significantly reduced at the acceptable cost of increased output voltage ripple [7]. According to the proven effects of SSFM, high DM-EMI amplitudes of boosting PFC converters with DCM control can be an apposite target. In [8] and [9], SSFM techniques were proposed for PFC rectifier applications based on integrated modulation of clock and signal generator.

EMI amplitudes in the research were significantly reduced, but waveform qualities were affected by the implemented SSFM due to the nonstraightforward frequency modulations.

Along with the trend, this letter aims to propose an SSFM suitable for DCM control in many boosting PFC converters. In Fig. 1, the desired spectrum of the proposed SSFM is shown. Under equal specifications of input–output, inductance, and power, the conventional DCM spectrum in black has much higher peak amplitudes than the distributed CRM spectrum in blue. Since the current mode of boosting PFC by DCM control can easily violate CCM when switching frequency is increased near the boundary, the proposed DCM spectrum aims to be located at the lower switching frequency region in red, which is called the down-spread spectrum technique [7]. Accordingly, reduction of switching losses is expected as an additional benefit.

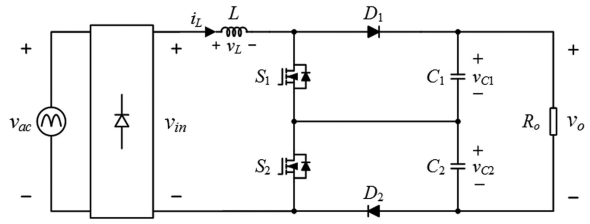

Fig. 2. TLB PFC converter.

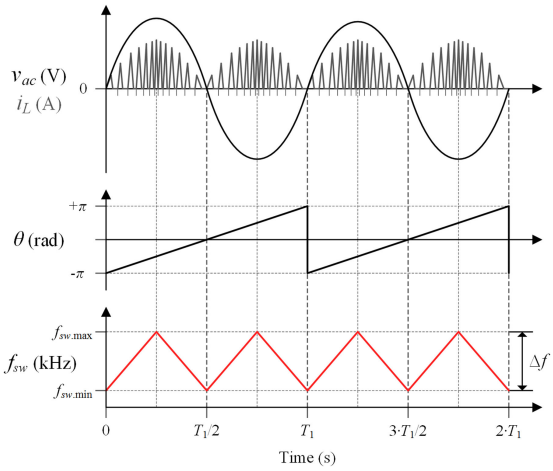

Fig. 3. Key waveforms of the proposed SSFM.

On top of the proposed SSFM, this letter utilizes three-level boost (TLB) PFC in Fig. 2 to achieve further EMI reductions. It can be mainly enabled by the proposed adaptive three-level current (ATC) scheme which is based on multilevel current-slope capability of TLB PFC [10]. Thus, two different DM-EMI reduction approaches are collaborated as follows.

1) Proposed SSFM technique: Distribute EMI spectrum.
2) Proposed ATC scheme: Minimize inductor current ripple.

This letter includes operation principles of the proposed methods, equations, implementation, and experimental results.

II. Proposed SSFM With ATC Scheme

A. Proposed SSFM

Fig. 3 shows key waveforms of the proposed SSFM for DCM boosting PFCs founded on general phase-locked-loop (PLL) control of ac input voltage [11]. From PLL control, angle θ of ac input is extracted to produce linearized switching-frequency distribution during ac line period T_1. Minimum and maximum frequencies are designed to locate at zero-crossing and peak input voltages, respectively. By doing so, the down-spread spectrum in Fig. 1 can be realized. The proposed frequency distribution in Fig. 3 can be formulated by (1) in terms of θ

$$f_{sw} = \big|\big|\theta| - \pi/2\big| - \pi/2\big| \cdot (2/\pi) \cdot \Delta f + f_{sw.\min} \quad (1)$$

where Δf is the frequency range of SSFM and $f_{sw.\min}$ is the minimum frequency limit, respectively. The minimum switching frequency is usually set above audible range while the maximum frequency of SSFM should be designed with considerations of switching losses, DCM operations, and hardware capabilities. With the proposed SSFM, conventional two-level DCM current

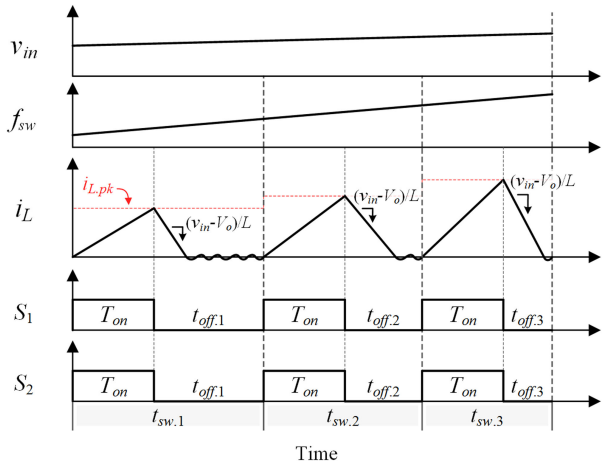

Fig. 4. Conventional DCM scheme with the proposed SSFM.

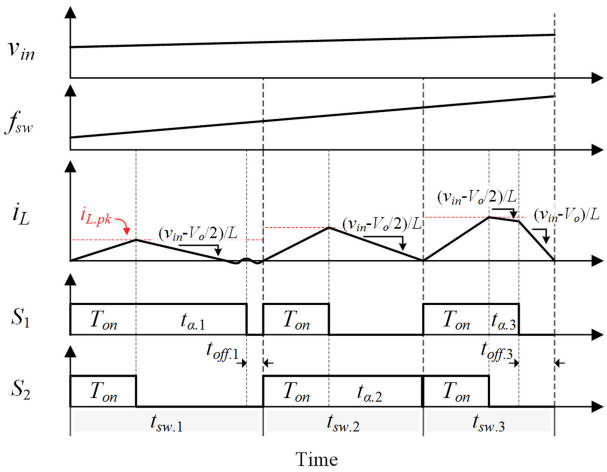

Fig. 5. Proposed ATC scheme with the proposed SSFM.

modulation can be used as Fig. 4. ON-time duration $T_{\rm on}$ is resulted from slow-dynamic compensator for v_o and remains almost constant during line cycles [4]. With a properly designed compensator, two-level DCM operations in Fig. 4 can be obtainable not only by TLB PFC, but also by two-level boosting PFC topologies (e.g., conventional boost PFC, dual boost PFC, and totem-pole boost PFC).

B. Proposed ATC Scheme for SSFM

With the proposed SSFM, DM-EMI amplitudes of DCM control can be significantly reduced. However, with TLB PFC, there remain chances to reduce EMI noises further. In general, multilevel feature is exploited to improve waveform qualities (e.g., THD) in ac–dc rectifiers and dc–ac inverters. From this standpoint, three-level current-slope capability of TLB can bring additional degrees-of-freedom to the proposed SSFM. In Fig. 5, key waveforms of the proposed ATC scheme are depicted. The main concept is adding an adaptive single-switch ON-time t_α in each switching cycle to get three-level current modulation. Depending on the input voltage level, inductor current can be both DCM and CRM forms, as shown in Fig. 5. Toggling of switch conduction for t_α between S_1 and S_2 is to mitigate asymmetry and output voltage unbalance.

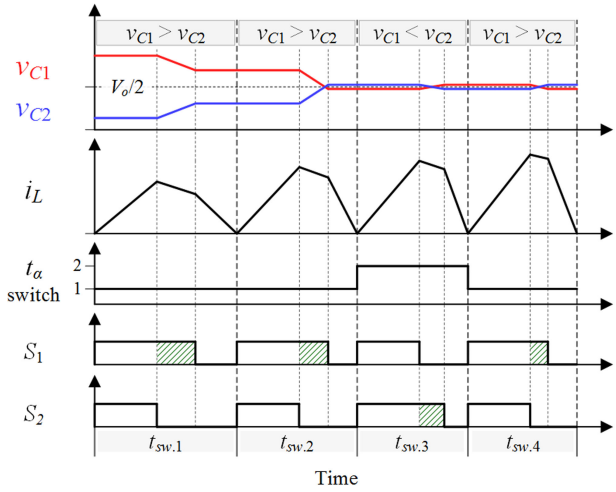

Fig. 6. Output voltage-balancing method in the proposed ATC scheme.

Under the assumption of equal input–output voltages, power, and inductance, average input currents of two-level DCM and ATC schemes can be equal only when the areas of inductor currents in each switching cycle are matched to each other. Since the duration of nonzero inductor current in Fig. 5 is longer than that in Fig. 4, it is reasonable to expect lower peak current from the proposed ATC scheme. Mathematically, the average $T_{\rm on}$ by the two-level DCM scheme is proven to be (2) by [1] and average $T_{\rm on}$ by proposed ATC scheme can be derived as (3) under equal power delivery assumption as follows:

$$T_{\rm on.2L} = \frac{t_{sw}}{V_{\rm in.}pk}\sqrt{\frac{2\pi f_{sw} L P_o}{\int_0^{\pi}\frac{\sin^2\theta}{\left(1-\frac{V_{\rm in.}pk}{v_o}|\sin\theta|\right)}d\theta}} \tag{2}$$

$$T_{\rm on.3L} = \left(\frac{v_o}{v_o - V_{\rm in.rms}}\cdot\frac{T_{\rm on.2L}}{t_{sw}}\right)\cdot T_{\rm on.2L} \tag{3}$$

where $V_{\rm in.}pk$ is the peak of input voltage and $V_{\rm in.rms}$ is the rms value of input voltage, respectively. Since $T_{\rm on.3L}$ is shorter than $T_{\rm on.2L}$ in most cases, lower peak current can be expected by $i_{L.}pk = (v_{\rm in}/L)\cdot T_{\rm on}$. In other words, the proposed ATC scheme can bring additional reductions of DM-EMI amplitudes in a different way, compared to the proposed SSFM itself. While the proposed SSFM distributes concentrated EMI energies to wide-range frequency spectrum, the proposed ATC scheme directly minimizes inductor current ripple and corresponding DM-EMI amplitudes. The feature of proposed ATC scheme is distinctively achievable by none other than TLB topology.

Although the toggling function of conducted switch for t_α in Fig. 5 is applied to the proposed ATC scheme, voltage balancing between v_{C1} and v_{C2} cannot be guaranteed. It is because the ac input and switching frequency conditions keep changing for line cycle T_1 so that asymmetric charging/discharging amounts of C_1 and C_2 are unavoidable. Thus, a balancing method that can be equipped with the proposed ATC scheme is devised as Fig. 6. The principles are as follows. The setup has sampling frequency set higher than $f_{sw.\max}$; 1) v_{C1} and v_{C2} are measured and higher voltage is defined as v_h; 2) higher voltage cell's switch is chosen

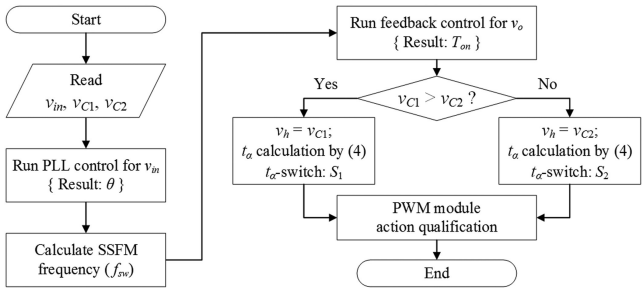

Fig. 7. Flowchart of the proposed SSFM with ATC scheme.

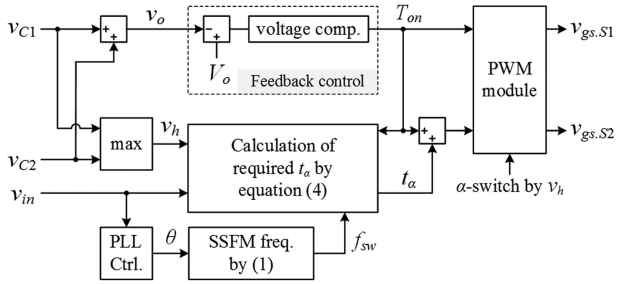

Fig. 8. Flowchart of the proposed SSFM with ATC scheme.

to be conducted in t_α period for discharging; and 3) required t_α in a cycle which can be calculated by the following is applied to the selected switch through pulsewidth-modulation (PWM) module

$$t_\alpha = \frac{(v_o - v_{\rm in})\cdot t_{sw} - v_o\cdot T_{\rm on}}{v_h}. \tag{4}$$

The solution in (4) reflects all the real-time input–output voltages and unbalanced conditions in order to achieve quadrangular CRM-shared current waveforms as close as possible; correspondingly, minimized inductor current ripple and DM-EMI amplitudes can be achieved under given switching frequency specifications. By the steps 1)–3) in each sampling cycle, TLB PFC with the proposed SSFM and ATC scheme can get balanced outputs; the flowchart of one sampling routine is summarized in Fig. 7. The entire control block diagram for the proposed SSFM and ATC scheme is also drawn in Fig. 8, visualizing the feedback path of $T_{\rm on}$ and feedforward process for t_α, respectively.

III. Experimental Results

For verifying the proposals, a 300-W TLB PFC prototype was built and tested with the specifications in Table I; the laboratory setup is shown in Fig. 9. Conditions 110 $\rm V_{rms}$ and 300 W are chosen for spectrum analysis because the combination of low input voltage and full load induces the largest DM-EMI.

In Fig. 10, steady-state waveforms of the proposed SSFM and ATC scheme are presented. The switching frequency varies between 25–35 kHz with input voltage variation. Zoom-in inductor currents in Fig. 10(b) show good agreement with the proposed ATC scheme in Fig. 5. Depending on the input level, TLB operates both in DCM and CRM forms with reduced peak currents which are direct root causes of DM-EMI amplitudes.

TABLE I
EXPERIMENTAL SPECIFICATIONS

Input voltage	110 V_{rms}
Output voltage	400 V
Load	60–300 W (20–100%)
Switches (S_1, S_2)	IPW60R041P6 (C_{oss}=310 pF, $R_{ds,on}$=41 mΩ)
Diodes (D_1, D_2)	C4D10120D (v_F=1.4 V)
Inductance (L)	230 μH
Capacitance (C_1, C_2)	470 μF
Digital controller	Texas instruments TMS320F28377D
SSFM frequency	25–35 kHz
Sampling frequency	40 kHz
EMI spectrum analyzer	Agilent N9320B

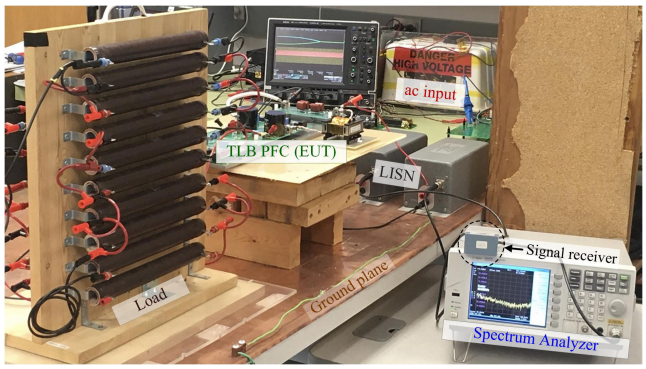

Fig. 9. EMI measurement setup.

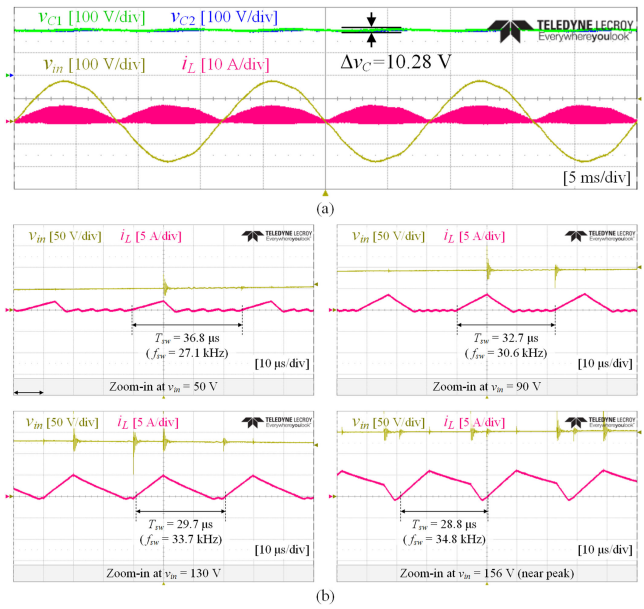

Fig. 10. Experimental results. (a) Steady state. (b) Zoom-in by input voltage.

In Fig. 11, the proposed SSFM based on ATC scheme is tested with and without voltage-balancing method. Before activating the balancing, 176 V unbalance existed. But, after activation, the unbalance is effectively resolved.

In Fig. 12, the measured DM-EMI results are shown by the control method. Around the switching frequency region, the proposed SSFM can reduce peak amplitudes by 12.7 dBμV

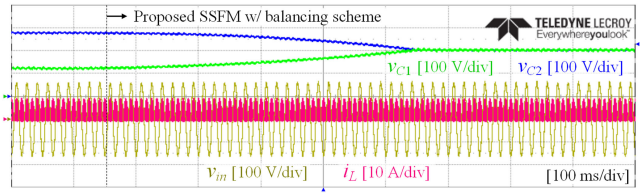

Fig. 11. Experimental results of voltage-balancing scheme.

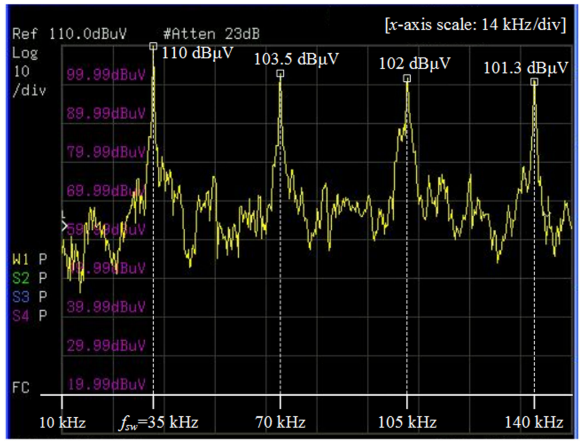

(a)

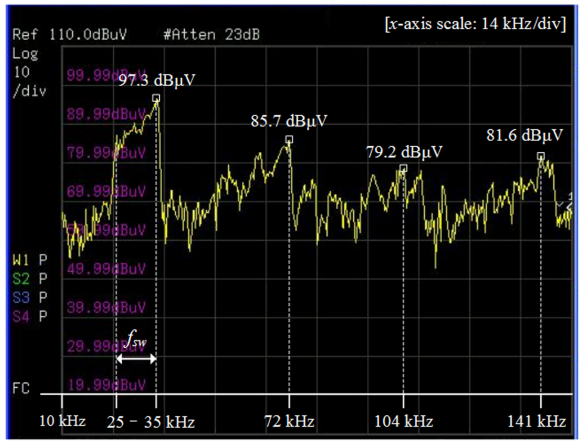

(b)

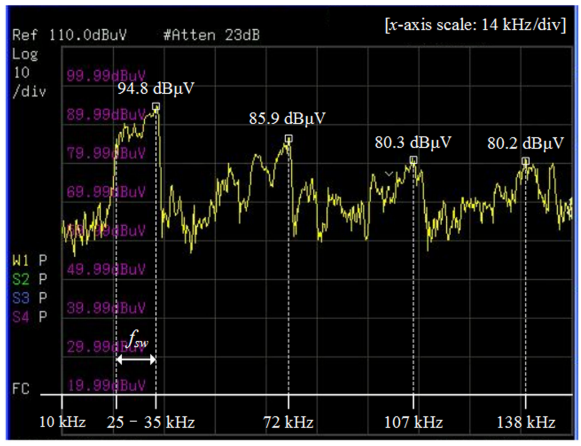

(c)

Fig. 12. DM-EMI measurement results by control method. (a) Fixed-frequency DCM. (b) Proposed SSFM. (c) Proposed SSFM with ATC scheme.

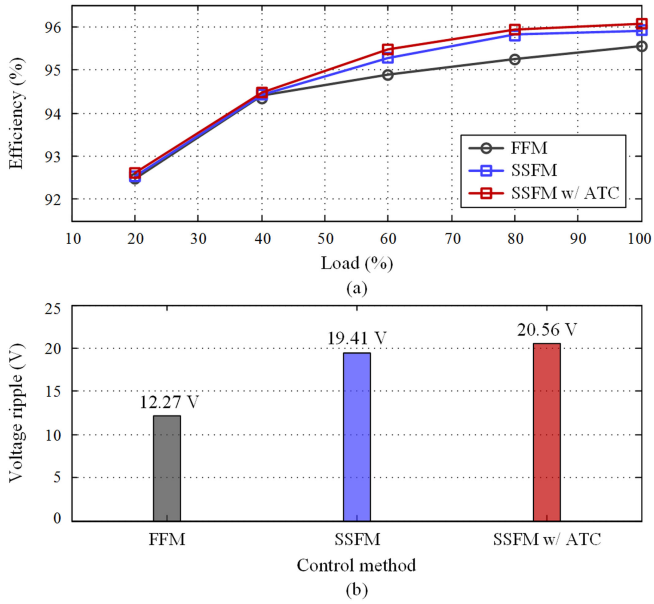

Fig. 13. Measurement by control method. (a) Efficiency. (b) Voltage ripple.

than fixed-frequency DCM, by the principle of distributing EMI-related energies on the frequency spectrum. The proposed ATC scheme can also bring further reduction by 2.5 dBμV by minimizing the inductor current ripple under given conditions of frequency, power, and voltages. Reduction effects are repeatedly found in integer multiples of switching frequencies and those patterns in the higher frequency region will be helpful for reducing filter sizes and fulfilling EMI standards.

In Fig. 13, measured efficiency and output voltage ripple are plotted. The proposed SSFM based on down-spectrum is rewarded with efficiency improvement by 0.43% on average than fixed-frequency modulation (FFM), and the proposed ATC scheme brings additional 0.12% increment on average. As mentioned in Section I, increased output voltage ripple is a tradeoff of the proposed SSFM. The results show that 7.14 and 8.28 V increments were measured from SSFM and SSFM with the ATC scheme, respectively.

IV. Conclusion

This letter proposes an SSFM technique for DCM boosting PFC converters including TLB topology to reduce DM-EMI amplitudes originated from high inductor current ripple and peak. To remain in DCM, down-spectrum-based frequency distribution is adopted to the SSFM and the reduction of switching losses is given as secondary benefit. On top of the proposed SSFM, this letter devises a novel ATC scheme for TLB PFC. The concept of adaptive single-switch ON-time brings further reductions of current ripple and EMI amplitudes by forming inductor current in quadrangular CRM shape, especially at the peak of input voltage. In summary, it can be noted that while the SSMF technique intentionally distributes EMI spectrum, the ATC scheme directly reduces inductor current ripple, which are main root causes of DM-EMI noises. Therefore, a collaboration of the two different EMI-reduction approaches can bring the lowest EMI amplitudes. Experimental results verify that the proposed SSFM and ATC scheme can improve EMI noises and efficiency at the cost of output voltage ripple increment.

References

[1] K. Yao, W. Hu, Q. Li, and J. Lyu, "A novel control scheme of DCM boost PFC converter," *IEEE Trans. Power Electron.*, vol. 30, no. 10, pp. 5605–5615, Oct. 2015.

[2] K. Yao, L. Li, H. Tang, C. Mao, and K. Chen, "Optimum boundary inductance control concerning limited PF for a DCM boost PFC converter," *IEEE Trans. Power Electron.*, vol. 35, no. 1, pp. 443–454, Jan. 2020.

[3] J. Kim and G. Moon, "Minimizing effect of input filter capacitor in a digital boundary conduction mode power factor corrector based on time-domain analysis," *IEEE Trans. Power Electron.*, vol. 31, no. 5, pp. 3827–3836, May 2016.

[4] Q. Ji, X. Ruan, L. Xie, and Z. Ye, "Conducted EMI spectra of average-current-controlled boost PFC converters operating in both CCM and DCM," *IEEE Trans. Ind. Electron.*, vol. 62, no. 4, pp. 2184–2194, Apr. 2015.

[5] H. Park, M. Kim, and J. Jung, "Spread spectrum technique to reduce EMI emission for an LLC resonant converter using a hybrid modulation method," *IEEE Trans. Power Electron.*, vol. 33, no. 5, pp. 3717–3721, May 2018.

[6] H. Park, S. Jeong, M. Kim, J. Kim, and J. Jung, "Spread spectrum technique for decreasing EM noise in high-frequency APWM HB resonant converter with reduced EMI filter size," *IEEE Trans. Power Electron.*, vol. 34, no. 11, pp. 10845–10855, Nov. 2019.

[7] F. Pareschi, R. Rovatti, and G. Setti, "EMI reduction via spread spectrum in DC/DC converters: State of the art, optimization, and tradeoffs," *IEEE Access*, vol. 3, pp. 2857–2874, 2015.

[8] D. Stepins, "An improved control technique of switching-frequency-modulated power factor correctors for low THD and high power factor," *IEEE Trans. Power Electron.*, vol. 31, no. 7, pp. 5201–5214, Jul. 2016.

[9] D. Stepins and J. Huang, "Effects of switching frequency modulation on input power quality of boost power factor correction converter," *Int. J. Power Electron. Drive Syst.*, vol. 8, no. 2, pp. 882–899, Jun. 2017.

[10] M. Lee, J. Kim, and J. Lai, "Digital-based critical conduction mode control for three-level boost PFC converter," *IEEE Trans. Power Electron.*, vol. 35, no. 7, pp. 7689–7701, Jul. 2020.

[11] J. Choe *et al.*, "Controller and EMI filter design for modular front-end solid-state transformer," in *Proc. IEEE Appl. Power Electron. Conf. Expo.*, Mar. 2018, pp. 188–192.